PRELIMINARY EVALUATION OF FeCrAl CLADDING FOR ACCIDENT TOLERANT FUEL CONCEPTS

J.D. HALES and K.A. GAMBLE

August 2015

PRELIMINARY EVALUATION OF FeCrAl CLADDING FOR ACCIDENT TOLERANT FUEL CONCEPTS

J.D. HALES and K.A. GAMBLE

August 2015

Idaho National Laboratory
Idaho Falls, Idaho 83415

http://www.inl.gov

PRELIMINARY EVALUATION OF FeCrAl CLADDING FOR ACCIDENT TOLERANT FUEL CONCEPTS

INL/EXT-15-36423

J.D. HALES, K.A. GAMBLE

Fuels Modeling and Simulation Department, Idaho National Laboratory
P.O. Box 1625, Idaho Falls, ID 83415, USA

ABSTRACT

Since the accident at the Fukushima Daiichi Nuclear Power Station, enhancing the accident tolerance of light water reactors (LWRs) has become an important research topic. In particular, the community is actively developing enhanced fuels and cladding for LWRs to improve safety in the event of accidents in the reactor or spent fuel pools. Fuels with enhanced accident tolerance are those that, in comparison with the standard UO2-zirconium alloy system, can tolerate loss of active cooling in the reactor core for a considerably longer time period during design-basis and beyond design-basis events while maintaining or improving the fuel performance during normal operations and operational transients. This report presents early work in developing thermal and mechanical models for FeCrAl, a proposed cladding material. BISON, the finite element-based fuel performance code in development at Idaho National Laboratory, was used to compare results from normal operation conditions with UO2/Zr-4 behavior. In addition, sensitivity studies are presented for evaluating the relative importance of material parameters such as elastic constants and thermal conductivity in order to provide guidance on future experiments for this material.

1.   Introduction

In March 2011, a magnitude 9.0 earthquake struck off the coast of Japan. The earthquake and the associated tsunami resulted in thousands of deaths, hundreds of thousands of damaged buildings, and a cost estimated to be in the hundreds of millions of dollars.

One consequence of the tsunami was the flooding of backup power generators at the Fukushima Daiichi Nuclear Power Station. The loss of power to coolant systems led to high temperatures, zircaloy oxidation, hydrogen production, melted fuel, and hydrogen explosions. As a result, a massive cleanup effort is underway at Fukushima Daiichi. The economic impacts, both those directly related to the cleanup and those affecting the nuclear energy sector generally, are significant.

Following the disaster, efforts to develop nuclear fuels with enhanced accident tolerance were begun by many nations, corporations, and research institutes. In the United States, the Department of Energy's Office of Nuclear Energy accelerated research on this topic as part of its Fuel Cycle Research and Development (FCRD) Advanced Fuels Campaign (AFC). One product of this work is *Light Water Reactor Accident Tolerant Fuel Performance Metrics* [1], a report by AFC that outlines a set of metrics that can be used to guide selection of promising accident tolerant fuel (ATF) concepts. Furthermore, [1] specifies that a down-selection is to occur in the 2016-2017 timeframe, at which time the program will move from a proof-of-

concept stage to a proof-of-principle stage and continue research and development on a small set of concepts.

Given the aggressive development schedule, it is impossible to perform a comprehensive set of experiments to provide material characterization data. Therefore, the AFC plans to utilize computational analysis tools in an effort to understand the proposed materials.

The Nuclear Energy Advanced Modeling and Simulation (NEAMS) program in DOE has for some time been developing computational analysis tools. These include BISON [2-4] and Marmot [5], analysis tools tailored to nuclear fuel at the engineering scale and grain scale, respectively. Recently, NEAMS has introduced what it calls High Impact Problems (HIPs) into its program plan. These HIPs are intended to make a significant advance in a particular area of nuclear power research in a short period of time (3 years or less). NEAMS has chosen an ATF project, which emphasizes utilizing BISON and Marmot to model proposed materials, as its first HIP.

This paper reviews initial work on modelling ATF concepts. The following section reviews BISON and the multiscale materials modelling approach involving Marmot that will be used to investigate novel materials. We then review FeCrAl as a cladding material, as well as a computational study involving this material. We conclude with a summary and a review of upcoming work.

2.   BISON and Multiscale Materials

BISON is a multidimensional nuclear fuel performance analysis code capable of 1D, 2D, and 3D simulations. It is applicable to engineering scale analysis of LWR fuel, TRISO-coated fuel particles, and metal fuels. Typically, the partial differential equations that BISON solves are the energy and solid mechanics equations for temperature and displacements, respectively. BISON's capabilities include a selection of fuel and cladding thermal and mechanical material models, fission gas release, thermal and mechanical contact, evolving gap conductivity and pressure, axial and radial power scaling, fuel densification and swelling, and other models. Due to the evolution of gap size between fuel and cladding in a light water reactor, solving the energy and mechanics equations in a fully-coupled manner is very important. It is also possible to run BISON coupled with a neutronics code [6].

Many of the material models in BISON are empirical. These models rely on curve-fitting equations to describe material behaviour in regimes spanned by experiments. These models are efficient and have been used with success for many years in many fuel performance codes. However, these models suffer from the serious limitation that they are not applicable beyond the range of the experimental data.

Multiscale modelling is an approach that may be able to extend the useful range of materials models. The approach is to begin with lower length scale models and simulations and then use the knowledge gained to develop new models at higher length scales. The modelling may begin with atomistic simulations that, for example, provide insight into thermal conductivity for a given material. This information can be used at the grain level in a package such as Marmot. Marmot can model grain evolution and other phenomena using input data from the atomistic simulations. The behaviour at the Marmot level may be homogenized for use at the engineering scale (BISON) [7].

Given the desire to place a lead test rod into a commercial reactor in a matter of a few years, it will not be possible to develop experiment-based empirical models describing the behaviour of the ATF concepts. Multiscale modelling will be used to provide guidance on the material behaviour where experimental data is sparse or non-existent.

3. FeCrAl

One proposed ATF cladding material for light water reactors is advanced oxidation-resistant iron alloys with a primarily iron-chromium-aluminum (Fe-Cr-Al) composition with the inclusion of other dopants such as molybdenum, yttrium, titatnium, and carbon. Commercial FeCrAl alloys under consideration for LWR cladding are Kanthal APMT [8], PM2000 [9], and MA956 [10] as investigated by Terrani et al. [11]. According to Terrani et al. oxide dispersions strengthened (ODS) alloys like the commercial ones listed above have increased creep resistance at high temperatures, which is a benefit over Zircaloy during design basis and beyond design basis accidents. Moreover, the oxidation rates of FeCrAl alloys are less than Zircaloy [11,12]. Additionally, the oxide layer that forms on the cladding prevents hydrogen ingress and hydride formation, which is prevalent in Zircaloy cladding. Thus, the increased risk of cladding failure due to the precipitation of circumferential hydrides during used fuel disposition is mitigated.

Some of the disadvantages and difficulties of using FeCrAl alloys as a cladding material include their lower melting points than Zircaloy. In addition research of various chromia (Cr_2O_3) forming steels found that the required chromium content for protective barrier formation in steam at 1200 ^{o}C is in excess of 20% [13]. These chromium concentrations would limit the irradiation performance of the alloy [11]. Furthermore, there is limited data on the mechanical properties of FeCrAl alloys and their durability under mechanical stresses and irradiation [12]. For example, the creep data available for MA956 and PM2000 produced by Wasilkowska et al. [14] is limited to a few select temperatures and is not presented in a manner that is easily implemented into BISON. This lack of data is an opportunity for multiscale modelling to help develop mechanistic material models. Sensitivity studies using these models can identify areas where further experiments are required.

To investigate the behaviour of FeCrAl cladding in a fuel performance setting and to identify areas where further research is required, a preliminary model of FeCrAl was added to BISON. The material model allows the selection of three different FeCrAl alloys: Kanthal APMT, PM2000 and MA956. Using the information provided in the datasheets available from the manufacturers of these alloys, the thermophysical properties including specific heat capacity, thermal conductivity, modulus of elasticity, Poisson's ratio, and coefficient of thermal expansion (CTE) are calculated as a function of temperature from the tabulated data. For temperatures between the tabulated points, linear interpolation is used. Linear interpolation was chosen because it ensures that the data points are accurately represented, but it is unclear whether linear interpolation is appropriate in every case. Temperatures outside the range of validity use the value at the nearest temperature for which data exists for lack of additional information. Note that the CTE data is provided as a mean value rather than instantaneous, and therefore to obtain the correct thermal strain the method by Niffenegger and Reichlin [15] needs to be employed.

When choosing a potential cladding material for accident tolerant applications, an understanding of the creep behaviour at normal operating and high temperatures as well as under irradiation conditions is of great importance. Of the commercial FeCrAl alloys of interest only MA956 has thermal creep data in a correlated format that allows easy input into BISON. No irradiation creep data exists for any of the FeCrAl alloys. The thermal creep correlation used for MA956 is a Norton law-based creep model proposed by Seiler et al. [16]:

$$\dot{\varepsilon} = \underbrace{A_0 \cdot \exp(\alpha T) \cdot \exp\left(-\frac{Q}{RT}\right)}_{A} \cdot \sigma^n \tag{1}$$

where Q is the activation energy, n is the creep exponent, α is a temperature coefficient, A_0 is the creep coefficient, T is the temperature in Kelvin, R is the ideal gas constant and σ is the effective stress in MPa. The creep behaviour is characterized by three distinct regimes

with independent sets of creep parameters. The transition from one regime to the next occurs at the critical stresses σ_{c1} and σ_{c2}, which are calculated by equating equation 1 for two of the regimes. For example, σ_{c1} is defined as

$$\sigma_{c1} = \left(\frac{A_1}{A_2}\right)^{\frac{1}{n_2-n_1}} \tag{2}$$

where $A_1(A_0, Q, \alpha, R, T)$ and n_1 are parameters in the range $\sigma < \sigma_{c1}$, and $A_2(A_0, Q, \alpha, R, T)$ and n_2 are parameters in the range $\sigma_{c1} < \sigma < \sigma_{c2}$, respectively. Table 1 lists the creep parameters of MA956 for the various stress regimes.

Table 1: Thermal creep parameters for FeCrAl alloy MA956

	A_0 [MPa^{-n}s^{-1}]	n [-]	Q [kJ/mol]	α [K^{-1}]
$\sigma < \sigma_{c1}$	78.978	4.9827	453	0.0
$\sigma_{c1} < \sigma < \sigma_{c2}$	3.466×10^{-124}	41.0	453	0.1
$\sigma > \sigma_{c2}$	8.68×10^{16}	5.2911	486	-0.0122

To demonstrate the behaviour of FeCrAl under light water reactor conditions, the current thermal, mechanical and creep materials for MA956 were used in a representative 2D axisymmetric example problem. The predicted behaviour was compared to the behaviour of a model using Zircaloy-4 as the cladding material. The geometric dimensions and operational parameters were adapted from Williamson et al. [2] and Metzger et al. [17]. The problem simulates a 10-pellet UO_2 fuel rodlet with cladding. The dimensions of the rodlet are typically of PWR fuel. The pellets had length and diameter of 11.9 mm and 8.2 mm, respectively. The cladding has a thickness of 0.56 mm for both materials for consistency, and a nominal initial radial gap of 80 µm was used. A second-order QUAD8 finite element mesh was used to approximate the geometry using 11 radial and 32 axial elements per pellet as illustrated in Figure 1. The cladding was modelled with 4 elements through the thickness and 326 elements axially.

A simple power history is applied to the fuel. It is assumed the power rises linearly over approximately three hours and then is held constant at 25 kW/m for approximately 3.2 years. A symmetric axial profile is applied the active fuel length of the rodlet such that the maximum power is applied at an axial position of 0.06162 m from the bottom of the fuel stack.
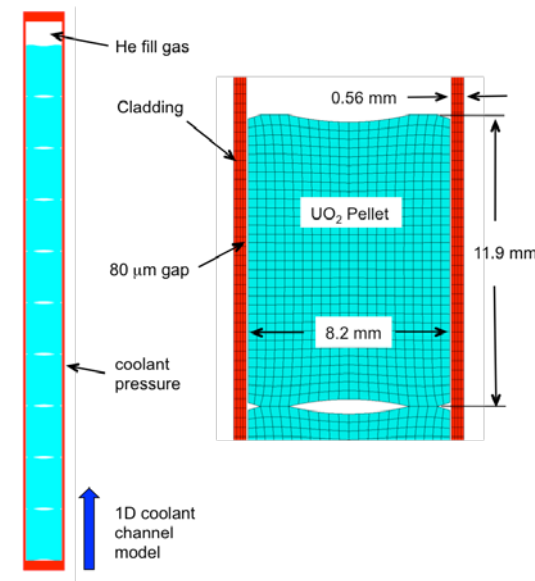

Figure 1: Geometry and mesh for the example problem. Adapted from references [2, 17].

A simple one-dimensional coolant channel model was used to calculate the convective heat transfer coefficient on the outside of the cladding. The operating conditions used are reproduced in Table 2.

Table 2: Operational parameters for the 2D axisymmetric example problem.

Linear average power (W/cm)	250
Fast neutron flux (n/m^{2}s)	7.5×10^{17}
Coolant pressure (MPa)	15.5
Coolant inlet temperature (K)	580
Coolant inlet mass flux (kg/m^2-s)	3800
Rod fill gas	Helium
Fill gas initial pressure (MPa)	2.0
Initial fuel density	95% theoretical
Fuel densification	1% theoretical
Burnup at full densification (MWd/kgU)	5

Comparisons between simulations of the example problem with Zircaloy-4 and MA956 are shown in Figure 2. Fig. 2a presents the comparison of fuel centreline, fuel surface and cladding inner surface temperatures as a function of burnup. It is observed from the beginning of irradiation that the fuel rodlet with MA956 cladding has higher fuel centerline and surface temperatures then the Zircaloy cladding rodlet. Significantly less creep is experienced by the MA956 resulting in the fuel-to-cladding gap remaining open for a longer duration leading to higher fuel temperatures. The inner cladding surface temperature remains relatively constant for both simulations. The point of fuel-to-cladding contact occurs at the points at which the slopes of the curves change (i.e. about 12 MWd/kgU and 38 MWd/kgU for the Zircaloy and MA956 rods respectively).

Since the MA956 rodlet experiences higher fuel temperatures, the fission gas released from the fuel grain boundaries to the plenum region is higher than the Zircaloy rodlet as illustrated in Figure 2b. However, the larger plenum and gap space within the fuel element due to less creep down of the cladding results in a lower pressure within the plenum. The magnitude of creep experienced by MA956 is very low at normal operating temperatures. It is, however, unclear what the effect irradiation creep would have on the behaviour of MA956 at these temperatures. In Zircaloy it is observed that thermal creep mechanisms are essentially negligible at normal operating temperatures (<600 $^{\circ}$C) where irradiation creep dominates, whereas at high temperatures (e.g. during a LOCA) thermal creep mechanisms are of greatest influence. Therefore, it is important to include irradiation effects of MA956 to see if the creep rate increases during normal operation as with Zircaloy.
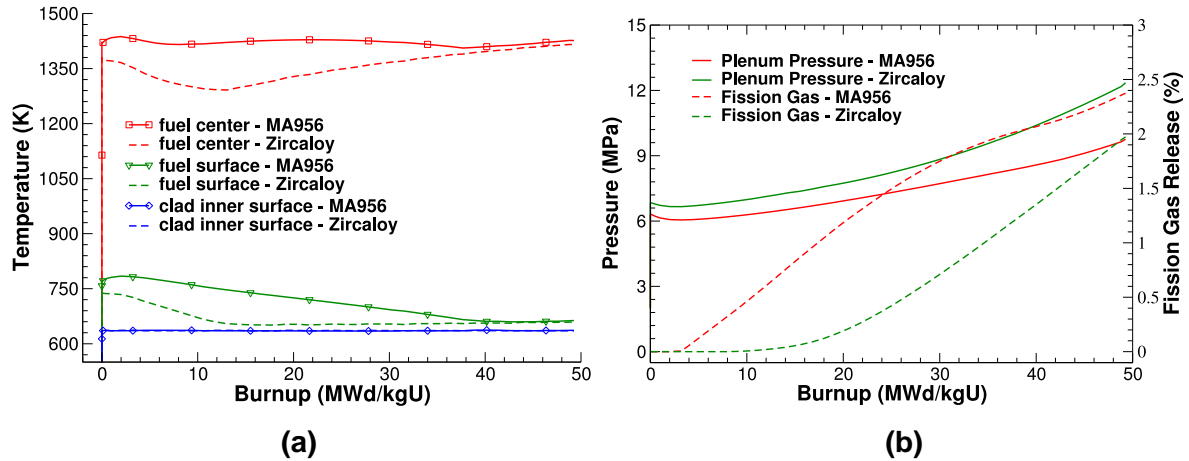
Figure 2: Comparisons between using MA956 or Zircaloy-4 cladding in the example problem for (a) fuel centerline, fuel surface, and clad inner surface temperatures, and (b) plenum pressure and fission gas released

While the example case above provides the nominal behaviour of MA956 cladding under normal operating conditions and highlights the limited creep experienced, there is still much not known about FeCrAl alloys. Moreover, the dimensions of an accident tolerant fuel rod are unclear. To gain a preliminary understanding of which mechanical and thermal properties, creep properties, and geometrical dimensions have the greatest influence on important rod properties such as the hoop stress and fuel centreline temperature, a sensitivity analysis was completed using Sandia National Laboratories' Dakota [18] software.

Starting with the nominal example problem with MA956 cladding, the Young's modulus, Poisson's ratio, thermal conductivity, radial gap width, and cladding thickness were varied by ± 10% to examine the effects of these parameters on hoop stress on the inner surface of the cladding and the fuel centreline temperature. Since the material properties vary as a function of temperature, a scale factor had to be used to properly vary these parameters. While varying the thermal creep parameters in equation 2 would be of interest, initial investigations indicated that for the example problem investigated here the negligible creep strain experienced does not have an affect on the stress results. Figure 3 shows main effects plots for the two output parameters of interest. The independent parameters (e.g., scale factors and geometry) were given 3 distinct values in a histogram form resulting in 243 simulations in the multidimensional parameter study. The information in a main effects plot is such that a point represents the mean value of the output parameter for all simulations at which the corresponding input parameter had that particular value. For example, the mean clad inner hoop stress is approximately -62.5 MPa for all simulations for which the Young's modulus was scaled by a factor of 0.9.

As expected it is imperative that the dimensions of an accident tolerant fuel rod be determined as the clad thickness and initial gap between the fuel and cladding have a strong influence on the stress state of the clad and the fuel centreline temperature as seen by the large slopes in the main effects plots for these parameters. The final centreline temperature is strongly influenced by the initial gap size. A larger initial gap results in higher temperatures because gap closure takes longer to occur. Similarly, a larger thickness means more material for the heat to pass through causing a slight increase in the centreline temperature. These plots confirm the expected behaviour when certain material parameters are varied.

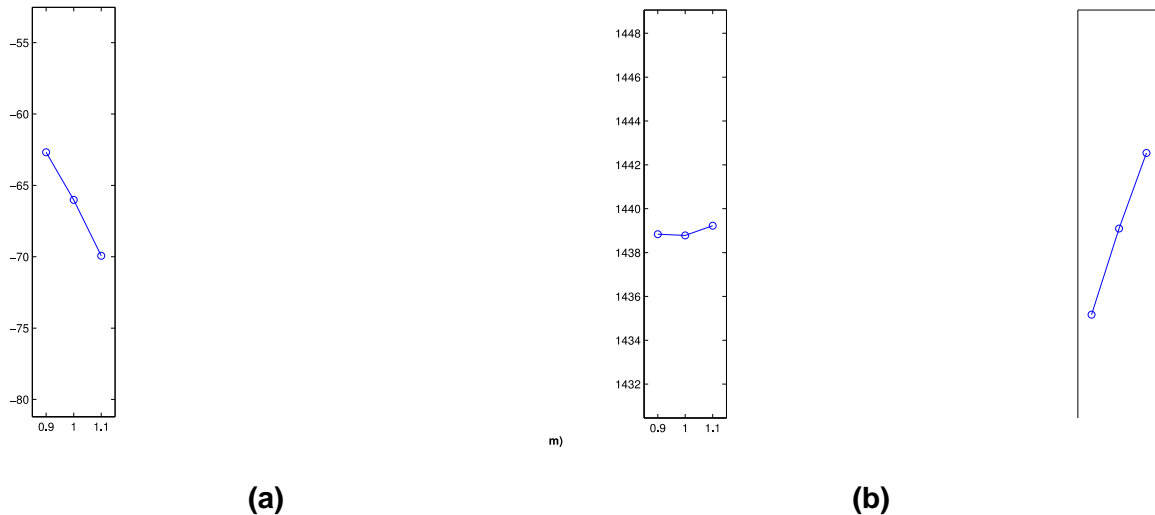**(a)**   **(b)**

Figure 3: Main effects plots analyzing the sensitivity of MA956 material parameters on the (a) clad inner hoop stress and (b) centerline temperature in the example problem at an axial location of 0.06162 m.

4.   Conclusions

FeCrAl is a leading ATF material. FeCrAl has several advantages over the traditional cladding material, Zircaloy. FeCrAl alloys experience significantly less creep, have slower oxidation rates, and do not absorb hydrogen from the coolant. Currently, a main concern of using of FeCrAl alloys is the lack of experimental and or lower length scale modelling to yield a greater understanding of the behaviour of these materials under normal operating and transient reactor conditions. Therefore, we need additional experimental data, along with multiscale modelling, to understand the thermophysical properties and irradiation creep behaviour of FeCrAl alloys. Sensitivity analyses were completed to illustrate the capability of investigating the effect of many input variables on the output of interest. We will work with the AFC to refine the geometry of the proposed ATF concepts and incorporate ongoing experimental data with lower length scale investigations to improve the quality of ATF modelling at the engineering scale.

5.   Acknowledgements

6.   References

[1] S. Bragg-Sitton, B. Merrill, M. Teague, L. Ott, K. Robb, M. Farmer, M. Billone, R. Montgomery, C. Stanek, M. Todosow, and N. Brown, "Advanced fuels campaign: enhanced LWR accident tolerant fuel performance metrics," INL/EXT-13-29957.

[2] R. L. Williamson, J. D. Hales, S. R. Novascone, M. R. Tonks, D. R. Gaston, C. J. Permann, D. Andrs, and R. C. Martineau, "Multidimensional multiphysics simulation of

nuclear fuel behavior," *J. Nucl. Mater.*, vol. 423, pp. 149–163, 2012. http://dx.doi.org/10.1016/j.jnucmat.2012.01.012.

[3] J. D. Hales, R. L. Williamson, S. R. Novascone, D. M. Perez, B. W. Spencer, and G. Pastore, "Multidimensional multiphysics simulation of TRISO particle fuel," *J. Nucl. Mater.*, vol. 443, pp. 531–543, 2013. http://dx.doi.org/10.1016/j.jnucmat.2013.07.070.

[4] J. D. Hales, S. R. Novascone, B. W. Spencer, R. L. Williamson, G. Pastore, and D. M. Perez, "Verification of the BISON fuel performance code," *Annals of Nuclear Energy*, vol. 71, pp. 81–93, 2014. http://dx.doi.org/10.1016/j.anucene.2014.03.027.

[5] M. R. Tonks, D. Gaston, P. C. Millett, D. Andrs, and P. Talbot, "An object-oriented finite element framework for multiphysics phase field simulations," *Comp. Mat. Sci.*, vol. 51, pp. 20–29, 2012.

[6] J. D. Hales, M. R. Tonks, F. N. Gleicher, B. W. Spencer, S. R. Novascone, R. L. Williamson, G. Pastore, D. M. Perez, "Advanced multiphysics coupling for LWR fuel performance analysis," *Annals of Nuclear Energy*, 2014. http://dx.doi.org/10.1016/j.anucene.2014.11.003.

[7] J. D. Hales, M. R. Tonks, K. Chockalingam, D. M. Perez, S. R. Novascone, B. W. Spencer, and R. L. Williamson, "Asymptotic expansion homogenization for multiscale nuclear fuel analysis," *Comp. Mat. Sci.*, vol. 99, pp. 290–297, 2015. http://dx.doi.org/10.1016/j.commatsci.2014.12.039

[8] Sandvik Kanthal APMT Datasheet, <http://kanthal.com/en/products/material-datasheets/tube/kanthal-apmt/>

[9] Schwarzkopf Plansee PM2000 Datasheet, <http://www.matweb.com/search/datasheet.aspx?matguid=21e9ec9a0de24b47bcf69ab11c375567&ckck=1.>

[10] Special Metals INCOLOY MA956 Datasheet, <http://www.specialmetals.com/documents/Incoloy%20alloy%20MA956.pdf>

[11] K. A. Terrani, S. J. Zinkle, and L. L. Snead, "Advanced oxidation-resistant iron-based alloys for LWR fuel cladding," *J. Nucl. Materi.,* vol. 448, pp. 420-435, 2014. http://dx.doi.org/10.1016/j.jucmat.2013.06.041I

[12] S. Dryepondt, B. A. Pint, and E. Lara-Curzio, "Creep behavior of commercial FeCrAl foils: Beneifical and detrimental effects of oxidation," *Materials Science and Engineering A,* vol. 550, pp. 10-18, 2012.

[13] B. A. Pint, K. A. Terrani, M. P. Brady, T. Cheng, J. R. Keiser, "High temperature oxidation of fuel cladding candidate materials in steam-hydrogen environments," *J. Nucl. Materi.,* vol. 440, pp. 420-427, 2013. http://dx.doi.org/10.1016/j.jnucmat.2013.05.047

[14] A. Wasilkowska, M. Bartsch, U. Messerschmidt, R. Herzog, A. Czyrska-Filemonowicz, "Creep mechanisms of ferritic oxide dispersion strengthened alloys," *J. Materi. Process. Tech.,* vol. 133, pp. 218-224, 2003.

[15] M. Niffenegger and K. Reichlin, "The proper use of thermal expansion coefficients in finite element calculations," *J. Nucl. Eng. Design,* vol. 243, pp 356-359, 2012. http://dx.doi.org/10.1016/j.nucengdes.2011.12.006

[16] P. Sieler, M. Bäker, and J. Rösler, "Variation of creep properties and interfacial roughness in thermal barrier coating systems," *Advanced Ceramic Coatings and Materials for Extreme Environments,* vol. 32, pp. 129-136, 2011.

[17] K. E. Metzger, T. W. Knight, and R. L. Williamson, "Model of U_3Si_2 Fuel System Using BISON Fuel Code," *Proc. Of ICAPP 2014,* Charlotte, USA, 2014.

[18] B. M. Adams, L. E. Bauman, W. J. Bohnhoff, K. R. Dalbey, M. S. Ebeida, J. P. Eddy, M. S. Eldred, P. D. Hough, K. T. Hu, J. D. Jakeman, L. P. Swiler, and D. M. Vigil, *"DAKOTA, A Multilevel Parallel Object-Oriented Framework for Design Optimization, Parameter Estimation, Uncertainty Quantification, and Sensitivity Analysis: Version 5.4 User's Manual,"* Sandia Technical Report SAND2010-2183, December 2009. Updated April 2013.